



The Influence of Annealing Temperature on Microstructure, Mechanical Properties, and Corrosion Resistance of Al-6Mg-0.4Mn-0.14Sc-0.12Zr Alloy Cold Rolling Plate

OPEN ACCESS

Edited by:

Antonio Caggiano,
Darmstadt University of
Technology, Germany

Reviewed by:

Martin Vlach,
Charles University, Czechia
Sung Bo Lee,
Seoul National University, South Korea
Sp Wen,
Beijing University of Technology, China

*Correspondence:

Feng Jiang
jfeng2@csu.edu.cn
Jianjun Zhang
zjjxjtu@163.com

Specialty section:

This article was submitted to
Structural Materials,
a section of the journal
Frontiers in Materials

Received: 10 January 2020

Accepted: 21 April 2020

Published: 17 June 2020

Citation:

Lu L, Jiang F, Liu J, Zhang J, Wang G,
Feng B, Tong M and Tang Z (2020)
The Influence of Annealing
Temperature on Microstructure,
Mechanical Properties, and Corrosion
Resistance of
Al-6Mg-0.4Mn-0.14Sc-0.12Zr Alloy
Cold Rolling Plate.
Front. Mater. 7:132.
doi: 10.3389/fmats.2020.00132

Liyong Lu^{1,2}, Feng Jiang^{1,3*}, Jiachen Liu⁴, Jianjun Zhang^{5*}, Guojun Wang², Bo Feng²,
Mengmeng Tong¹ and Zhongqin Tang¹

¹ School of Materials Science and Engineering, Central South University, Changsha, China, ² Northeast Light Alloy Co., Ltd., Harbin, China, ³ National Key Laboratory of Science and Technology for National Defense on High-strength Structural Materials, Central South University, Changsha, China, ⁴ School of Materials Science and Engineering, Taiyuan University of Science and Technology, Taiyuan, China, ⁵ Key Laboratory of Fluid and Power Machinery (Xihua University), Ministry of Education, School of Material Science and Engineering, Xihua University, Chengdu, China

An Al-6Mg-0.4Mn-0.14Sc-0.12Zr alloy with a low Sc content was developed. The mechanical properties and corrosion resistance of the Al-6Mg-0.4Mn-0.14Sc-0.12Zr alloy cold rolling plate which annealed at different temperatures were studied and discussed. Based on OM, SEM, EDS, and TEM techniques, the influence of annealing temperature on the microstructure of the alloy was studied. An Sc-free alloy was also developed as the control group. A comparison between the Sc-containing alloy and the control group was carried out on the mechanical properties and the microstructural characteristics for different processing conditions. In conclusion, when increasing annealing temperature, the corrosion resistance decreases first, and then increases. When annealed at 200°C for 2 h, Al₃Mg₂ phase is precipitated continuously along the grain boundary, leading to the lowest corrosion resistance. When annealed at 350°C for 2 h, the Al₃Mg₂ phase is not observed along the grain boundary, leading to a relatively high corrosion resistance. Moreover, the effective pinning of the grain boundaries by Al₃(Sc,Zr) particles constrains the recrystallization. As a result, a preferable combination performance of the Sc-containing alloy cold rolling plate can be obtained with the tensile strength of 437 MPa, the yield strength of 318 MPa, the elongation of 14.8%, and the corrosion resistance of 0.029 mm·a⁻¹. The research findings provide theoretical and experimental support for the industrial production of Al-Mg-Mn-Sc-Zr alloys with low Sc content.

Keywords: Al-6Mg-0.4Mn-0.14Sc-0.12Zr alloy, cold rolling plate, annealing process, mechanical properties, corrosion resistance

INTRODUCTION

Al-Mg series alloys have advantages, such as a high specific strength, good weldability, and good formability. Therefore, they are widely used in applications of aerospace, automobiles, vessels, etc. (Vargel et al., 2004; Polmear, 2005; Yong-yi et al., 2011; Gupta et al., 2012). Typically, increasing the Mg content improves the strength of Al-Mg alloys (Davis, 2001; Vargel et al., 2004; Polmear, 2005; Gupta et al., 2012). Whereas, there is a limitation for the alloys with a high Mg content. The tensile strength of the alloys gets close to a saturation point, about 440 MPa, in high Mg content of 7 wt% (Hua and Yue-e, 2001). Moreover, the corrosion resistance of the alloy decreases as the Mg content increases. The Al-Mg alloy with 7 wt% Mg content suffers from a low corrosion resistance. Besides, Al-Mg alloys with a high Mg content have a softening issue during annealing process. Some studies verified that Al-Mg alloys with a low Mg content ($Mg \leq 3.5\text{wt}\%$) had superior formability and corrosion resistance, which provided a new way for their development.

It was found that a small amount of Sc and Zr content could dramatically increase the overall performance of the alloys compared with that of the traditional alloys containing only Al and Mg (Pan et al., 2001; Yang et al., 2010; Chen et al., 2012a; Jia et al., 2012). The reason is that Sc and Zr contents not only improve the as-cast microstructure of the alloy, but also increases the recrystallization temperature of the alloy and enhances its sub-grain strengthening. Therefore, new Al-Mg-Sc-Zr series alloys have a higher strength and wider application prospect than the traditional Al-Mg alloys. The research on the processing technologies of Al-Mg-Sc-Zr series alloys has become popular recently (Nie et al., 2008; Du et al., 2010; Zhang et al., 2014; Huang et al., 2015; Vlach et al., 2017a,b; Yan and Hodge, 2017).

In recent years, properties, precipitation characteristics, and strengthening and toughening mechanisms of Al-Mg-Sc-Zr alloys were studied. The characteristics of $Al_3(\text{Sc,Zr})$ particles were presented and the strengthening method of Al-Mg series alloys was also illustrated (Nie et al., 2008; Du et al., 2010; Chen et al., 2012b; Vlach et al., 2012, 2015, 2017a,b, 2018; Meng et al., 2013; Buranova et al., 2017; Yan and Hodge, 2017). However, more research should be done on the influence of annealing temperature on both the mechanical properties and corrosion resistance of the Al-Mg-Sc-Zr alloy with low Sc content cold rolling plate and their correlation to their microstructures.

In this research, an Al-6Mg-0.4Mn-0.14Sc-0.12Zr (in mass fraction) alloy was casted with a low Sc (0.14 wt%) content. First, the microstructure of the Al-6Mg-0.4Mn-0.14Sc-0.12Zr alloy under cold rolling conditions was studied. Second, mechanical properties and corrosion resistance were tested on the alloy samples compared with those of the control group, Sc-free alloy, at different annealing temperatures. Their microstructural characterizations were also compared. The influence of $Al_3(\text{Sc,Zr})$ and $Al_3\text{Mg}_2$ particles on the microstructure of the alloy at different annealing temperatures were studied. The research findings provided theoretical and experimental support for the industrial production of Al-Mg-Mn-Sc-Zr alloys with low Sc content.

MATERIALS AND EXPERIMENT PROCEDURE

Two compositions of Al-Mg alloys were casted and tested. The Al-6Mg-0.4Mn-0.14Sc-0.12Zr alloy (Sc-containing alloy) was the main studying material and the Al-6Mg-0.4Mn-0.12Zr alloy (Sc-free alloy) was the control group. In order to simulate industrial casting conditions, large oblate ingots of the alloys were casted in sizes of $300 \times 1,500 \times 5,000$ mm. The ingots were treated by homogenization process and processed by hot rolling. As a result, thick alloy plates were obtained. They were further processed by multi-pass cold rolling to 3.5 mm plates with a 75% cold rolling reduction ratio. The chemical composition of the Sc-containing alloy was tested by photoelectricity spectroscopy, as shown in **Table 1**.

The samples in dimensions of $3.5 \times 300 \times 300$ mm were cut from the large rolling plates of the alloys. Annealing processes were conducted in a Nabertherm furnace. Annealing temperatures of 200, 280, 320, 350, 420, and 550°C and an annealing time of 2 h were selected for annealing of each cold rolled samples. The mechanical properties and microstructures of the prepared samples with two compositions were also tested at different annealing temperatures. The corrosion resistance of the Sc-containing alloy samples was also tested at different annealing temperatures.

An OLYMPUS DSX500 optical microscope (OM) and Tecnai G2 F20 ST transmission electron microscope (TEM) were used to observe and analyze the microstructural characteristics for cold rolled specimens at different annealing temperatures. A scanning electron microscope (SEM) with energy disperse spectroscopy (EDS) capability was also used.

The annealing specimens were grounded, polished, degreased by acetone, rinsed by distilled water, and air dried. The non-working surfaces were sealed by epoxy resin. The polarization curve was tested by an IM6ex electrochemical workstation. The three electrode system was used. Saturated calomel electrode was the reference electrode. The specimen was working electrode. Platinum plate was another working electrode. 3.5% NaCl neutral solution was chosen as the electrolyte.

Intergranular corrosion resistance was tested using ASTM G67 standard. Specific preparation procedure of the specimens was as follow: Cuboid specimens were cut from annealing plates. The dimension of the specimen was 50 mm in rolling direction, 6 mm in width direction, and the thickness of the rolling plate was 3.5 mm. Three specimens were tested for each annealing condition. Before testing, all the cutting surfaces of the specimens were grounded. The specimens were rinsed with distilled water. Subsequently, the specimens were dipped in 3.5% NaOH solution at a temperature of 80°C for 1 min and submerged in high concentration nitric acid for 30 s. Then, the specimens were

TABLE 1 | Chemical composition of the casted Sc-containing alloy (wt. %).

Mg	Mn	Sc	Zr	Ti	Be	Fe	Si	Al
6.054	0.394	0.138	0.119	0.027	0.0023	0.125	0.053	Bal

rinsed with distilled water, dried, and weighed. After the preparation procedure, specimens were submerged in 72% high concentration nitric acid at a temperature of 30°C for 24 h and weighed subsequently.

RESULTS

Mechanical Properties of Sc-Containing and Sc-Free Alloys

Figure 1 presents the influence of annealing temperature on the mechanical properties of the Sc-free alloy and the Sc-containing alloy. As shown in **Figure 1A**, when increasing the annealing temperature of both the two alloys, the tensile strength and yield strength decreases and the elongation increases. Moreover, at the same annealing temperature (including the cold rolling sample), the tensile strength and yield strength of the Sc-containing alloy are much higher than those of the Sc-free alloy. Besides, when even annealed at a high temperature of 350°C, a relatively high tensile and yield strength of the Sc-containing alloy remained at a relatively high level, which are also much higher than those of the Sc-free alloy. Therefore, adding small amounts of the Sc element effectively increases the strength of the alloy even when annealed at relatively high temperatures. In summary, comprehensively considering the strength and elongation of the alloy, the annealing process of 350°C/2 h is appropriate for the Sc-containing alloy. The tensile strength of 437 MPa and the yield strength of 318 MPa are obtained. Its elongation reaches 14.8%.

Microstructural Observations of Sc-Containing and Sc-Free Alloys

Figure 2 presents the microstructures of the cold rolling plates of both the Sc-free alloy and the Sc-containing alloys annealed at temperatures of 200, 350, and 420°C. The microstructure of the cold rolled Sc-free alloy specimen shows a typical straight fibrous deformation structure, as shown in **Figure 2A**. In contrast, the microstructure of the cold rolled Sc-containing alloy specimen exhibits a curved fibrous deformation structure, as shown in **Figure 2B**. The most frequently-occurring directions of the fibrous structures are in angles of 45 or 135° with respect to the rolling direction. These directions are matched well with the typical shear band direction.

For the Sc-free alloy annealed at a temperature of 200°C for 2 h, some recrystallized grains are clearly observed between the fibrous deformed grains, as shown in **Figure 2C**. For the Sc-free alloy annealed at a temperature of 350°C for 2 h, the fibrous deformed grains are broadened. The recrystallized grains are also distributed in the microstructure, as shown in **Figure 2E**. For the Sc-free alloy annealed at 420°C for 2 h, the original fibrous structures are completely consumed by equiaxed recrystallized grains. Some extremely coarse grains are observed, as shown in **Figure 2G**. However, for Sc-containing alloys annealed at temperatures of 200, 350, and 420°C, the fibrous structures and the shear bands can be observed distinctly. The only small difference is that the fibrous deformed structures are slightly coarsened with increasing annealing temperature, as shown in **Figures 2D,F,H**. It is verified that a substantial recrystallization

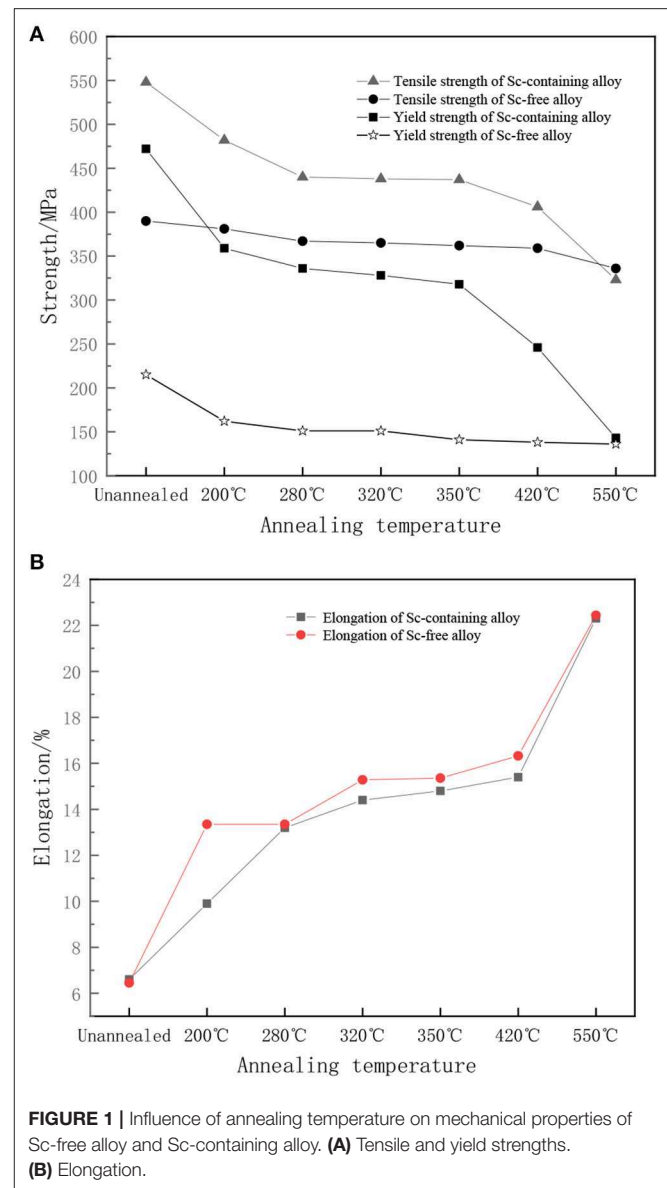


FIGURE 1 | Influence of annealing temperature on mechanical properties of Sc-free alloy and Sc-containing alloy. **(A)** Tensile and yield strengths. **(B)** Elongation.

does not occur in the microstructures of Sc-containing alloys annealed at temperatures of 200, 350, 420°C.

Intergranular Corrosion Resistance of Sc-Containing Alloy

Figure 3 shows the intergranular corrosion resistance of the Sc-containing alloy annealed at different temperatures using the weight loss method. The cold rolling sample and the samples annealed at temperatures above 280°C have good intergranular corrosion resistance. Their weight losses are <math>< 15 \text{ mg/mm}^2</math>. These samples are not sensitive to intergranular corrosion. However, the intergranular corrosion resistance of the alloy reaches the lowest value when annealed at a temperature of 200°C for 2 h. The weight loss of the specimen is around

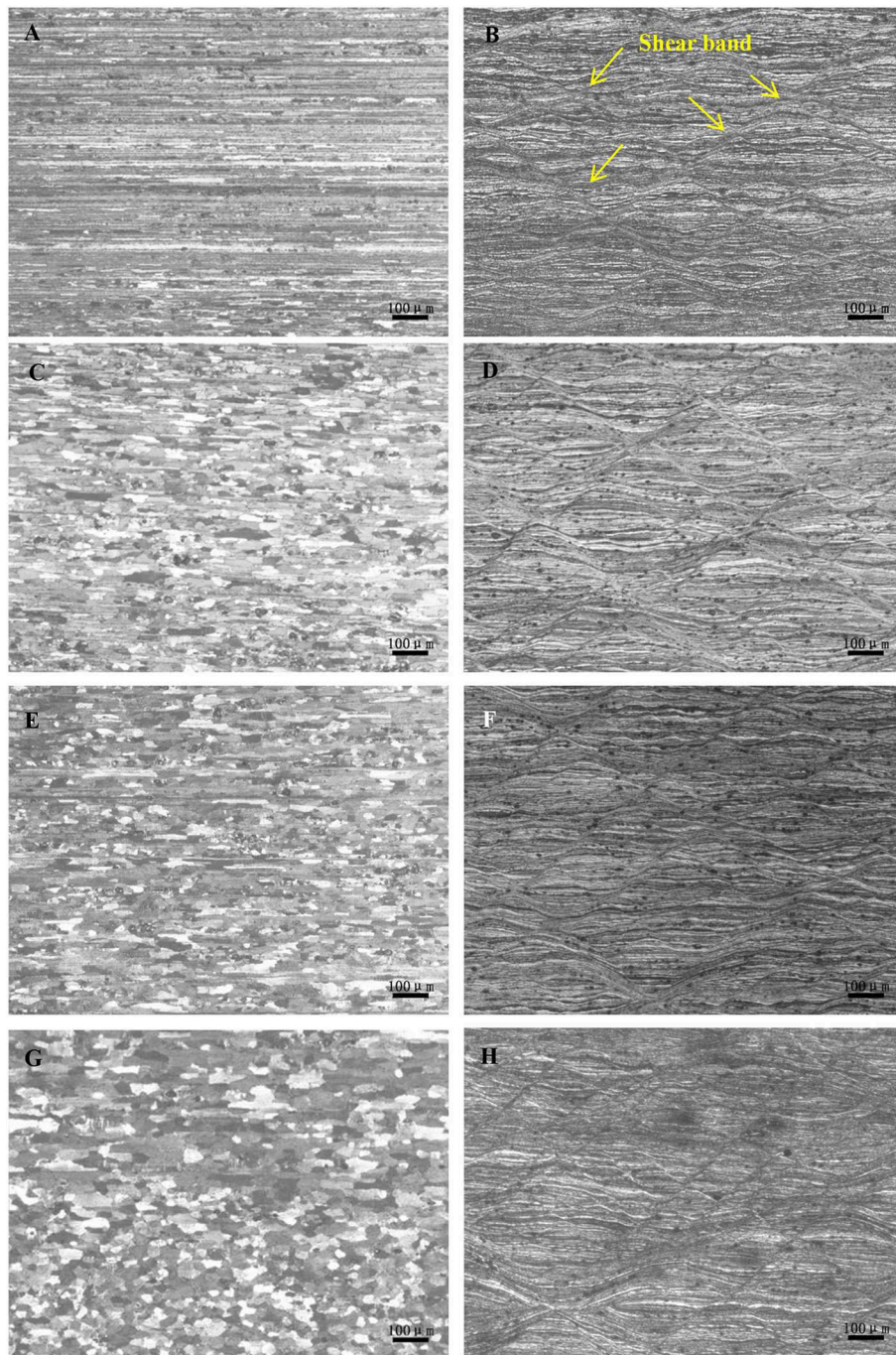


FIGURE 2 | Microstructures of the cold rolling plates of the Sc-free alloy and Sc-containing alloy annealed at different temperatures. **(A)** Sc-free, cold rolled; **(B)** Sc-containing, cold rolled; **(C)** Sc-free, 200°C anneal; **(D)** Sc-containing, 200°C anneal; **(E)** Sc-free, 350°C anneal; **(F)** Sc-containing, 350°C anneal; **(G)** Sc-free, 420°C anneal; **(H)** Sc-containing, 420°C anneal.

annealing process of 200°C/2 h is in the sensitive area of the intergranular corrosion.

As shown in **Figure 4**, polarization curves of the Sc-containing alloy at different annealing temperatures are presented. The polarization correlated parameters listed in **Table 2** are obtained

from fitting results of the specimens annealed at different temperatures. The corrosion rates in **Table 2** are calculated from Equation (1) Cao, 2008:

$$V = 3.27 \times 10^{-3} J_{\text{corr}} \times M/n\rho \quad (1)$$

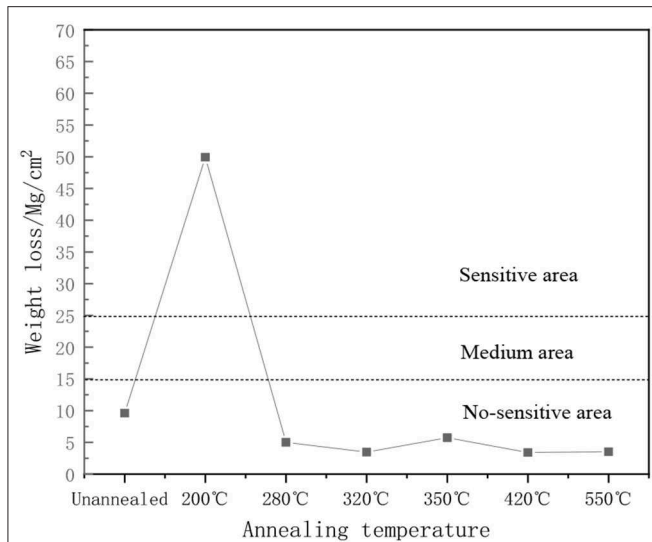


FIGURE 3 | The intergranular corrosion of the Sc-containing alloy annealed at different temperatures (including cold rolling sample) using the weight loss method.

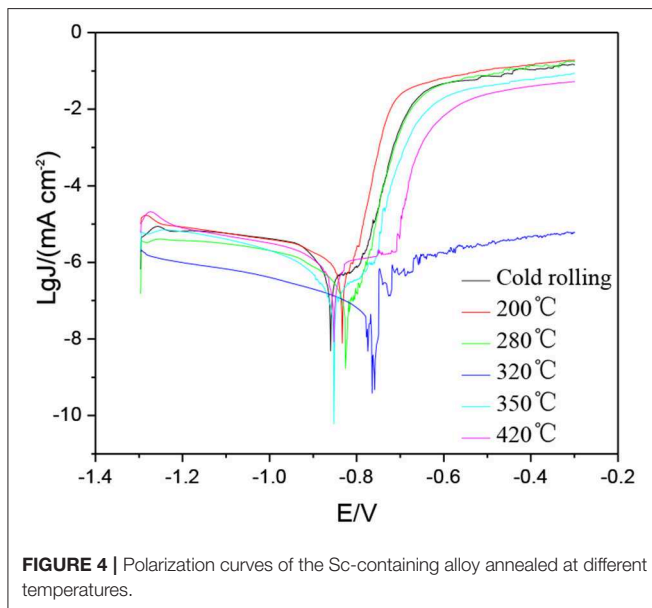


FIGURE 4 | Polarization curves of the Sc-containing alloy annealed at different temperatures.

where, J_{corr} is self-corrosion current density from fitting results ($\mu\text{A}\cdot\text{cm}^{-2}$); M is relative atomic mass of aluminum, $M = 27$; n is the valence of aluminum; and ρ is the density of aluminum, $\rho = 2.74 \text{ g/cm}^3$.

As shown in **Table 2**, when increasing annealing temperature, corrosion potential increases first, and then decreases. When annealed at a temperature of 200°C , the corrosion rate increases to the highest value, $0.486 \text{ mm}\cdot\text{a}^{-1}$. When further increasing annealing temperature, the corrosion rate decreases. When annealing temperature increases to 320°C , the annealed specimen has a high corrosion resistance, with the corrosion rate decreasing to $0.029 \text{ mm}\cdot\text{a}^{-1}$ and the corrosion potential increasing to -0.858 V .

TEM Observation of the Sc-Containing Alloy

TEM images of the cold rolling sample and the samples annealed at temperatures of 350 and 550°C are shown in **Figure 5**. **Figure 5A** shows that high density dislocations are generated under large deformation by the cold rolling process. Dislocation cells are formed by dislocation tangling. When annealed at a temperature of 350°C , the sub-grains are formed by the polygonization process, as shown in **Figure 5B**. When annealed at a temperature of 550°C , sub-grains are observed in local regions of the microstructure, as shown in **Figure 5C**. The sub-grains are pinned by dispersedly distributed sphere-shaped particles, $\text{Al}_3(\text{Sc,Zr})$ (Vlach et al., 2012; Meng et al., 2013; Buranova et al., 2017), as shown in **Figure 5D**.

Figure 6 shows the HAADF image from TEM and EDS analysis of the cold rolling plates at an annealing process of $200^\circ\text{C}/2 \text{ h}$. The phase that was interruptedly distributed along the grain boundary is analyzed by EDS, which is confirmed to be a Mn-rich phase, as shown in **Figures 6F,H**. The phase that distributed continuously along the grain boundary is tested by map scanning. The result shows that it is a Mg-rich phase, as shown in **Figures 6B–D**. Combined with their morphology features from the literature (Ding et al., 2020), the phase that distributed interruptedly along the grain boundary is Al_6Mn phase. The phase distributed continuously along the grain boundary is Al_3Mg_2 (β) phase. Due to a large amount of Al_3Mg_2 phase distributed along the grain boundary at an annealing process of $200^\circ\text{C}/2 \text{ h}$, the intergranular corrosion resistance of the alloy decreases significantly. Besides, the nano-scale sphere-shaped Sc-rich particle is also found close to the grain boundary, as shown in **Figure 6E**.

At an annealing process of $200^\circ\text{C}/2 \text{ h}$, a large amount of Al_3Mg_2 (β) phase is precipitated continuously along the grain boundary, as shown in **Figure 6A**. However, at an annealing process of $350^\circ\text{C}/2 \text{ h}$, β phase is not observed and the grain boundary is clear without the continuously distributed phase, as shown in **Figure 7**. Whereas, the small sphere-shaped particles are distinctly observed in **Figure 7**. As is shown in **Figure 5D**, these small sphere-shaped particles are confirmed to be $\text{Al}_3(\text{Sc,Zr})$ phase (Vlach et al., 2012; Meng et al., 2013; Buranova et al., 2017). As is known, dispersedly distributed $\text{Al}_3(\text{Sc,Zr})$ particles play the key role of pinning sites to constrain the dislocation slip and grain boundary migration, as shown in **Figures 7A,B**. As a result, at relatively high annealing temperatures, such as 350°C , the alloy (Sc-containing alloy) still has relatively high tensile strength, as shown in **Figure 1A**.

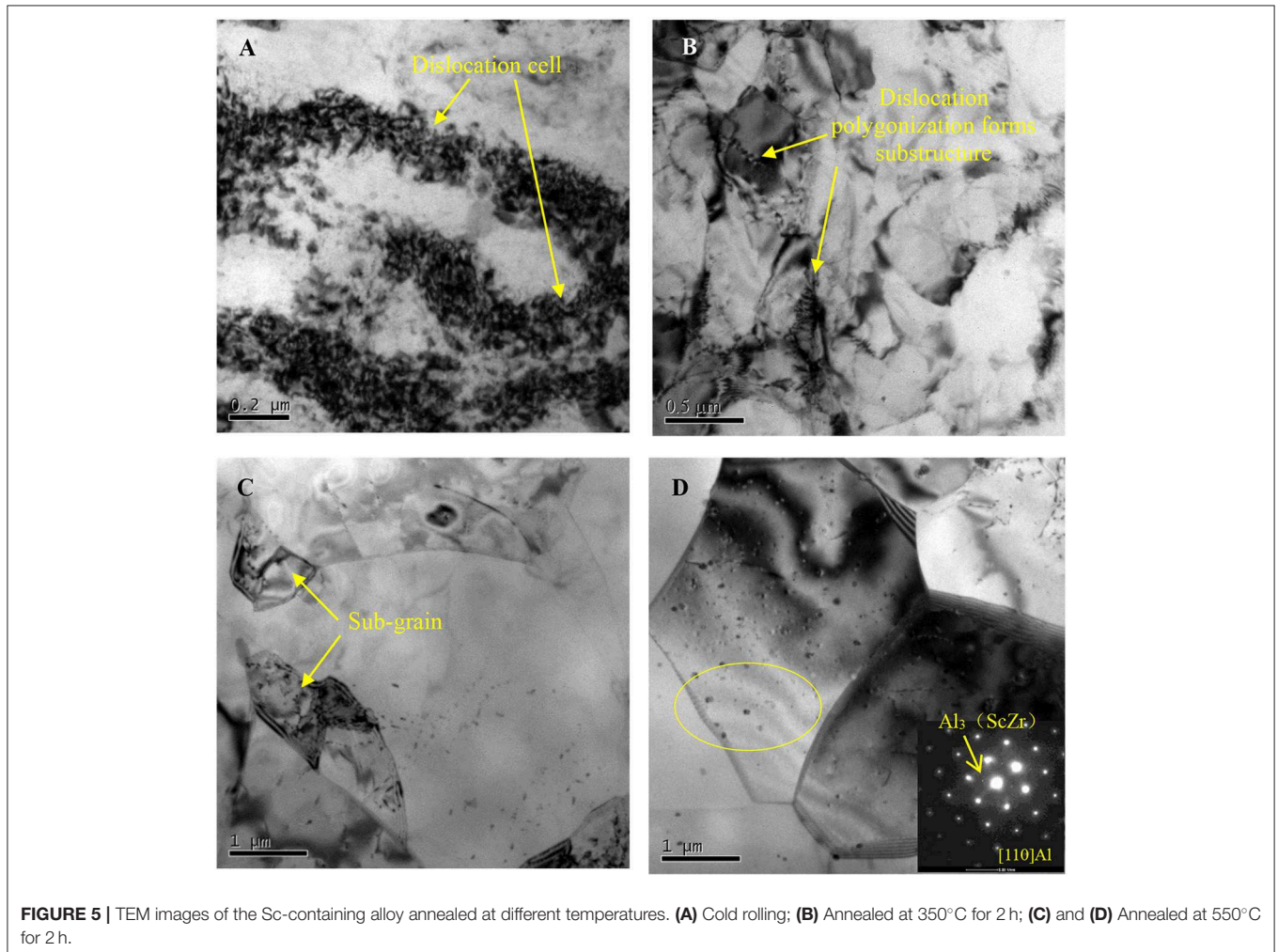
DISCUSSION

The Influence of Annealing Temperature on the Mechanical Properties of the Sc-Containing Alloy

As shown in **Figure 5A**, during cold rolling, high density dislocation tangling structures can be observed in the TEM image. The reason is that a mass of nano-scaled sphere-shaped $\text{Al}_3(\text{Sc,Zr})$ particles are dispersed with a size of around 20 nm in

TABLE 2 | Fitting results of the polarization curves of the Sc-containing alloy samples annealed at different temperatures.

Annealing temperature	Cold rolling	200°C	280°C	320°C	350°C	420°C
Self-corrosion potential/V	-0.876	-0.831	-0.823	-0.761	-0.858	-0.861
Self-corrosion current density/ $\mu\text{A}\cdot\text{cm}^{-2}$	8.921	45.231	8.314	4.911	2.672	1.196
Corrosion rate/ $\text{mm}\cdot\text{a}^{-1}$	0.096	0.486	0.089	0.053	0.029	0.013



the matrix. These large numbers of particles impede dislocation slip. Hence, during the cold rolling process, the work hardening of the alloy plate is obtained, increasing the strength (Du et al., 2010; Vlach et al., 2017a). However, the elongation of the alloy is decreased to 6.6%. Whereas, when increasing annealing temperature, recovery and recrystallization mechanisms occur in deformed microstructure. The tensile strength and yield strength of the alloy decreases, while elongation increases. It is interesting that a mass of $\text{Al}_3(\text{Sc,Zr})$ particles are dispersed in the matrix. The coherent boundary energy between $\text{Al}_3(\text{Sc,Zr})$ particles and matrix is low. Thus, these coherent boundaries are stable. As a result, $\text{Al}_3(\text{Sc,Zr})$ particles can impede dislocation slip and effectively pin the sub-boundary and grain boundary (Vlach et al., 2012; Meng et al., 2013; Buranova et al., 2017). It is difficult

for grains to grow even when annealed at high temperatures, as shown in **Figure 5C**. The dispersedly distributed $\text{Al}_3(\text{Sc,Zr})$ particles decreases softening rate while recrystallization occurs during the annealing process. In sum, a superior combination of the tensile strength of 437 MPa, the yield strength of 318 MPa, and the elongation of 15% is obtained when annealed at 350°C for 2 h.

The Influence of Annealing Temperature on Intergranular Corrosion Resistance of the Sc-Containing Alloy

The driving force of the corrosion electrochemistry of the alloy is the potential difference between the grain boundary

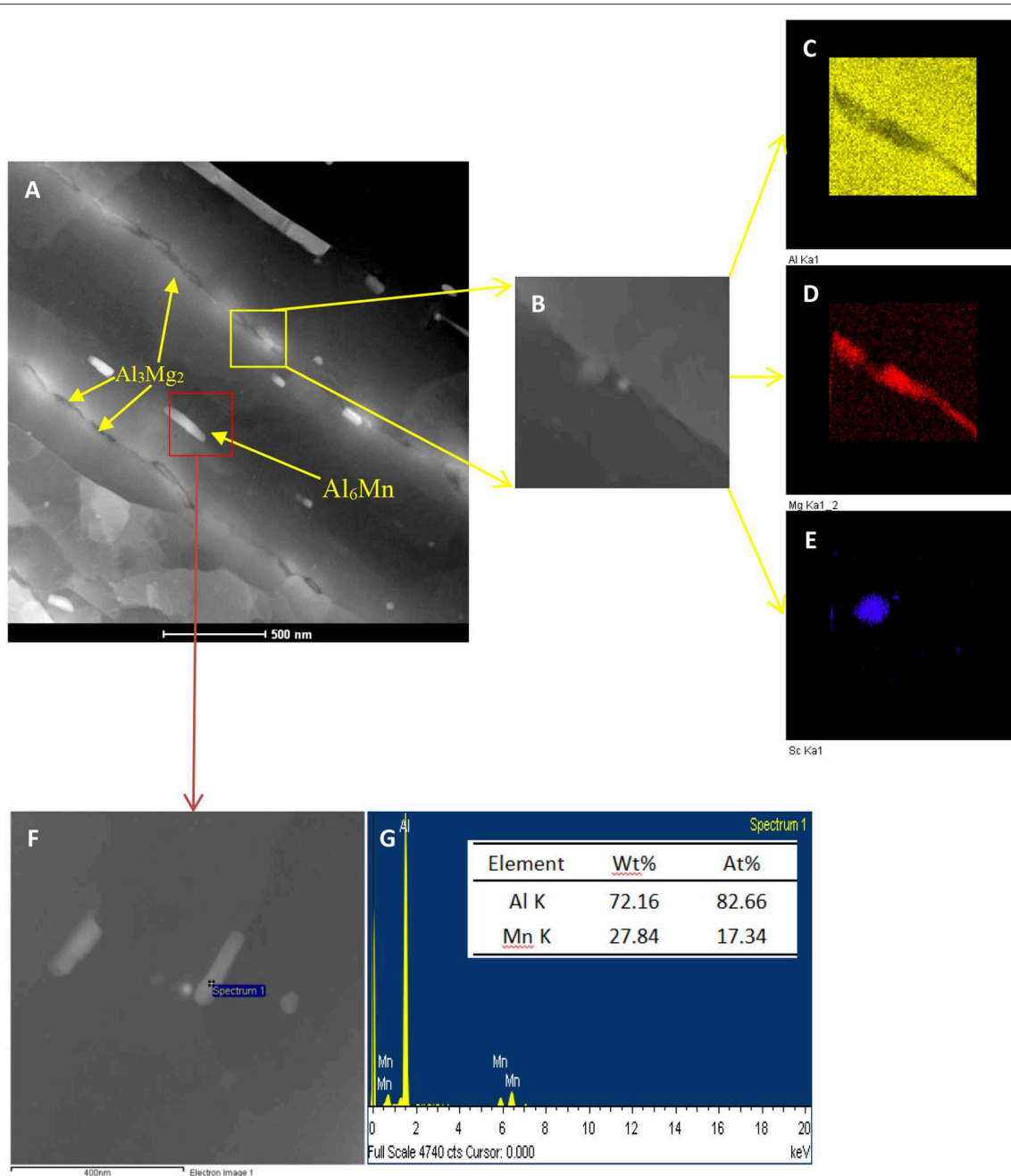


FIGURE 6 | HAADF image from TEM and EDS analysis of the Sc-containing cold rolling plates annealed at 200°C for 2 h. (A) HAADF image; (B) zoom in image; (C) detection of Al by map scanning; (D) detection of Mg by map scanning; (E) detection of Sc by map scanning; (F) zoom in image; (G) EDS analysis.

and the matrix of the grain. The chemical potential of the precipitation is different from that of the matrix and depleted zone near the grain boundary. The grain boundary contains defects, impurities, and high concentrations of alloying elements. Hence, the grain boundary is more active than that of the matrix, resulting in its more negative electrode potential. In general, the matrix is considered as the cathode and the grain boundary is considered as the anode. A microbattery system is formed and the intergranular corrosion occurs.

The phases of $\alpha(Al)$, $\beta(Mg_2Al_3)$, Al_6Mn , and $Al_3(Sc,Zr)$ are presented in the alloy, as shown in **Figures 5D, 6C–G**. As β phase is distributed along the grain boundary, the intergranular corrosion is developing along the grain boundary. Due to the higher electric potential of β phase than that of the Al-Mg-Mn alloy matrix, β phase can be resolved in a corrosive medium in the first place. The corrosion situation of the alloy in a corrosive solution mainly depends on the distribution, size, and amount of β phase (Wang et al., 2012).

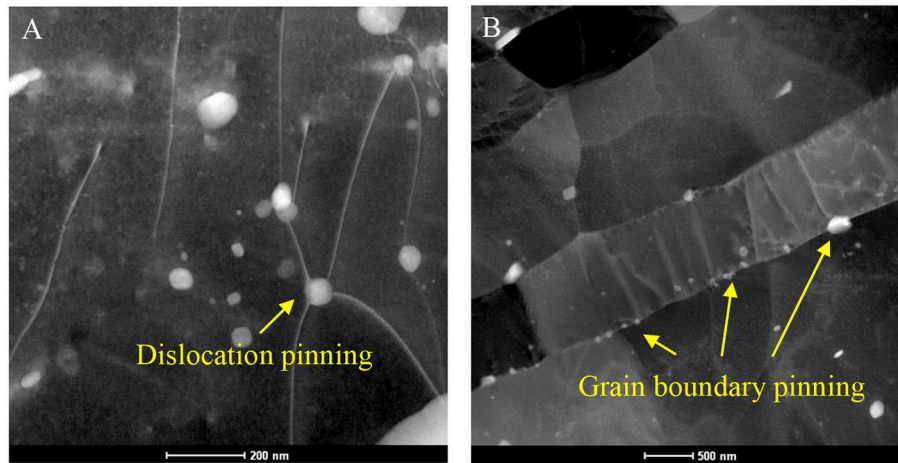


FIGURE 7 | HAADF images of the Sc-containing alloy cold rolling plate annealed at 350°C for 2 h. **(A)** pinning dislocation; **(B)** pinning grain boundary.

Research has verified that an Al alloy with Mg content no more than 3.5% does not exhibit thin layers of intergranular precipitation networks annealed at any temperatures after cold rolling process (Brown, 1972). According to the Al-Mg binary phase diagram, at 200°C, the saturation solubility of Mg in α solid solution is 3.1%. Below 200°C, the saturation solubility of Mg is 3.0%. However, for a high Al-Mg alloy, such as the alloy (6.0% Mg) in this research, thin layers of β phase can be precipitated along the grain boundary during storing for 2–4 years or 200°C/2h annealing. Interestingly, when the alloy with a high Mg content is annealed higher than 280°C, β phase is not observed along the grain boundary. Therefore, the issue of the intergranular β phase precipitation can be resolved.

CONCLUSIONS

- (1) An Al-6Mg-0.4Mn-0.14Sc-0.12Zr alloy with a low Sc content is developed. During the cold rolling process of the alloy, a large amount of shear bands is formed. The dislocation density is high in the local shear band region.
- (2) At the same annealing temperature, the tensile strength and yield strength of the Sc-containing alloy are much higher than those of the control group, the Sc-free alloy. Adding small amounts of Sc element effectively increases the strength of the annealed alloy.
- (3) When increasing the annealing temperature, the strength of the alloy plate slightly decreases and its elongation increases. Nano-sized $\text{Al}_3(\text{Sc,Zr})$ particles, which are dispersedly precipitated in the matrix, hinder the dislocation slip and the grain boundary migration, and hence, impede recrystallization, leading to the significant increase of recrystallization temperature of the cold rolling plate.
- (4) When increasing annealing temperature, the corrosion resistance decreases first, and then increases. When

annealed at 200°C for 2 h, Al_3Mg_2 (β) phase is precipitated continuously along the grain boundary, leading to a potential difference between β phase and the matrix. The lowest corrosion resistance is obtained. When annealed at 350°C for 2 h, the Al_3Mg_2 phase is not observed along the grain boundary, leading to a relatively high corrosion resistance. Only the $\text{Al}_3(\text{Sc,Zr})$ particles dispersedly precipitated in the matrix are observed.

- (5) When the Al-6Mg-0.4Mn-0.14Sc-0.12Zr alloy cold rolling plate is annealed at 350°C for 2 h, the best combination performance can be obtained with the tensile strength of 437 MPa, the yield strength of 318 MPa, the elongation of 14.8%, and the corrosion resistance of $0.029 \text{ mm}\cdot\text{a}^{-1}$. The research findings provide theoretical and experimental support for the industrial production of the Al-Mg-Mn-Sc-Zr alloy with a low Sc content.

DATA AVAILABILITY STATEMENT

The raw data supporting the conclusions of this article will be made available by the authors, without undue reservation, to any qualified researcher.

AUTHOR CONTRIBUTIONS

LL designed the experiment, analyzed the data and wrote the draft of the paper. FJ advised the research work, provided the research equipment and revised the paper. JL analyzed the data and revised the paper. JZ provided the research funding and revised the paper. GW provided the research equipment and collected the data. BF analyzed the data. MT and ZT conducted the experiment and collected the data.

REFERENCES

- Brown, B. F. (1972). Stress-Corrosion cracking in high strength steels and in titanium and aluminum alloys. Washington, DC: Naval Research Laboratory, 184–190.
- Buranova, Y., Kulitskiy, V. A., Peterlechner, M., Mogucheva, A. A., Kaibyshev, R., Divinski, S. V., et al. (2017). Al₃(Sc,Zr)-based precipitates in Al-Mg alloy: effect of severe deformation. *Acta Mater.* 124, 210–224. doi: 10.1016/j.actamat.2016.10.064
- Cao, C. (2008). *Principles of Electrochemistry of Corrosion*. Beijing: Chemical Industry Press.
- Chen, Q., Pan Q-Lin, W., Ying, Z. Z.-Y., Zhou, J., and Liu, C. (2012a). Microstructure and mechanical properties of Al-5.8Mg-Mn-Sc-Zr alloy after annealing treatment. *J. Central South University* 19, 1785–1790. doi: 10.1007/s11771-012-1208-x
- Chen, Q., Pan, Q.-L., Wang, Y., Peng, H., Zhang, Z.-, and Ye, Yin, Z.-,Min. (2012b). Effects of minor scandium and zirconium on microstructure and mechanical properties of Al-Mg-Mn alloys. *Chinese J. Nonferrous Metals* 22, 1555–1563.
- Davis, J. R. (2001). *Surface Engineering for Corrosion and Wear Resistance*. Materials Park, OH: ASM International. 29–35.
- Ding, Y., Wu, X., Gao, K., Huang, C., Xiong, X., Huang, H., et al. (2020). The influence of stabilization treatment on long-term corrosion resistance and microstructure in Er and Zr containing 5083 aluminum alloy. *Mater. Characterization* 161, 110–143. doi: 10.1016/j.matchar.2020.110143
- Du, G., Yang, W., Y., De-S., and Rong, L.-J. (2010). Precipitation behaviors of primary phases in Al-Mg-Sc-Zr alloy. *Chinese J. Nonferrous Metals* 20, 1083–1087.
- Gupta, R. K., Sukiman, N. L., Cavanaugh, M. K., Hinton, B. R. W., Hutchinson, C. R., and Birbilis, N. (2012). Metastable pitting characteristics of aluminium alloys measured using current transients during potentiostatic polarisation. *Electrochim. Acta.* 66, 245–254. doi: 10.1016/j.electacta.2012.01.090
- Hua, Z., and Yue-e, W., (2001). The effect of annealing temperature on exfoliation corrosion of Al-7.0Mg. *Aluminium Fabrication*. 24, 32–35.
- Huang, H., Feng, J., Zhou, J., Lili, W., Qu, J., and Lele, L. (2015). Effects of Al₃(Sc,Zr) and shear band formation on the tensile properties and fracture behavior of Al-Mg-Sc-Zr Alloy. *J. Mater. Eng. Perform.* 24, 4244–4252. doi: 10.1007/s11665-015-1748-y
- Jia, Z.-H., Royset, J., Solberg, J. K., and Lie, Q. (2012). Formation of precipitates and recrystallization resistance in Al-Sc-Zr alloys. *Trans. Nonferrous Metals Soc. China* 22, 1866–1871. doi: 10.1016/S1003-6326(11)61399-X
- Meng, Y., Zhao, Z.-H., and Cui, J.-Z. (2013). Effect of minor Zr and Sc on microstructures and mechanical properties of Al-Mg-Si-Cu-Cr-V alloys. *Trans. Nonferrous Metals Soc. China* 23, 1882–1889. doi: 10.1016/S1003-6326(13)62673-4
- Nie, B., Yin, Z.-M., Jiang, F., Jiang, C.-L., and Cong, F.-G. (2008). Influence of stabilizing annealing on tensile property and exfoliation corrosion resistance of Al-Mg-Sc alloy. *Trans. Mater. Heat Treat.* 29, 58–61.
- Pan, Q.-L., Yin, Z.-M., Zhou, J.-X., Chen, X.-M., and Zhang, C.-F. (2001). Effects of minor Sc of Al-Mg Alloy. *Acta Metallurgica Sinica.* 37, 749–753.
- Polmear, I. J. (2005). *Light alloys[M]. 4th Edn*. Oxford: Butterworth-Heinemann, 97–204. doi: 10.1016/B978-075066371-7/50007-4
- Vargel, C., Jacques, M., and Schmidt, M. P. (2004). *Corrosion of Aluminium*. Amsterdam: Elsevier, 61–69. doi: 10.1016/B978-008044495-6/50009-4
- Vlach, M., Cížek, J., Smola, B., Melikhova, O., Vlček M., Kodetov, V., et al., (2017a). Heat treatment and age hardening of Al-Si-Mg-Mn commercial alloy with addition of Sc and Zr. *Mater. Characterization* 129, 1–8. doi: 10.1016/j.matchar.2017.04.017
- Vlach, M., Cizek, J., Smola, B., Stulíková I., Hruška, P., Kodetova, V., et al. (2018). Influence of dislocations on precipitation processes in hot-extruded Al-Mn-Sc-Zr alloy. *Int. J. Mater. Res.* 109, 583–592. doi: 10.3139/146.111654
- Vlach, M., Smola, B., Stulíková I., Kodetova, V., Kudrnova, H., Malek, J., et al. (2017b). Phase Transformations and Recrystallization in Cold-Rolled Al-Mg-Sc-Zr Alloy Prepared by Powder Metallurgy. *Defect Diffusion Forum.* 380, 161–166. doi: 10.4028/www.scientific.net/DDF.380.161
- Vlach, M., Stulíková I., Smola, B., Kekule, T., Kudrnova, H., Kodetova, V., et al. (2015). Annealing effects in hot-deformed Al-Mn-Sc-Zr alloys. *Kovove Mater.* 53, 295–304. doi: 10.4149/km_2015_5_295
- Vlach, M., Stulíková, I., Smola, B., Piesova, J., Cisarova, H., Danis, S., et al. (2012). Effect of cold rolling on precipitation processes in Al-Mn-Sc-Zr alloy. effect of cold rolling on precipitation processes in Al-Mn-Sc-Zr alloy. *Mater. Sci. Eng. A* 548, 27–32. doi: 10.1016/j.msea.2012.03.063
- Wang, Y., Pan Q.-L., and Peng, H. (2012). Effect of annealing temperature on mechanical and corrosion properties of Al-Mg-Sc alloy. *J. Mater. Sci. Eng.* 30, 913–918.
- Yan, J., and Hodge, A. M. (2017). Study of β precipitation and layer structure formation in Al 5083: The role of dispersoids and grain boundaries. *J. Alloys Compounds* 703, 242–250. doi: 10.1016/j.jallcom.2017.01.360
- Yang, F.-B., Liu, E.-K., Jun, X., Zhang, Z.-F., and Shi, L.-K. (2010). Hot-cracking susceptibility of (Sc, Zr, Er)-microalloyed Al-5Mg filler metals. *Chinese J. Nonferrous Metals* 20, 620–627.
- Yong-yi, P., Zhi-min, Y., Xue-feng, L., Qing-lin, P., and Zhen-bo, H. (2011). Microstructure and properties of friction stir welded joints of Al-Mg-Sc alloy sheets. *Rare Metal Mater. Eng.* 40, 201–205. doi: 10.1016/S1875-5372(11)60015-5
- Zhang, W., Xing, Y., Jia, Z.-H., Yang X.-F., Liu, Q., and Zhu, C.-L. (2014). Effect of minor Sc and Zr addition on microstructure and properties of ultra-high strength aluminum alloy. *Trans. Nonferrous Metals Soc. China* 24, 3866–3871. doi: 10.1016/S1003-6326(14)63544-5

Conflict of Interest: LL, GW, and BF were employed by the company, Northeast Light Alloy Co.

The remaining authors declare that the research was conducted in the absence of any commercial or financial relationships that could be construed as a potential conflict of interest.

Copyright © 2020 Lu, Jiang, Liu, Zhang, Wang, Feng, Tong and Tang. This is an open-access article distributed under the terms of the Creative Commons Attribution License (CC BY). The use, distribution or reproduction in other forums is permitted, provided the original author(s) and the copyright owner(s) are credited and that the original publication in this journal is cited, in accordance with accepted academic practice. No use, distribution or reproduction is permitted which does not comply with these terms.